



Reducing pitfall risk using seismic inversion and rock physics analysis

Andrea Damasceno, Elita de Abreu and Viviane Farroco – Petrobras - E&P-EXP/GEOF/EGPI
Josimar Silva- Data and Consulting Services/Schlumberger

Copyright 2011, SBGf - Sociedade Brasileira de Geofísica

This paper was prepared for presentation during the 12th International Congress of the Brazilian Geophysical Society held in Rio de Janeiro, Brazil, August 15-18, 2011.

Contents of this paper were reviewed by the Technical Committee of the 12th International Congress of the Brazilian Geophysical Society and do not necessarily represent any position of the SBGf, its officers or members. Electronic reproduction or storage of any part of this paper for commercial purposes without the written consent of the Brazilian Geophysical Society is prohibited.

Abstract

Four Partial stacked time migrated seismic data were inverted for absolute and relative impedance and Vp/Vs ratio, generating also as additional results Poisson ratio and Shear Impedance. Additionally, rock physics analysis using available well logs was made trying to discriminate oil from background (water sands and other lithologies). Integrating both information, it was possible to discriminate amplitude anomalies related to oil saturation from lithologic anomalies.

Introduction

Conventionally in oil industry many reservoirs are identified using amplitude anomalies, e.g. bright spots and dim spots (Castagna, 1993). According to Bacon (2003), seismic amplitudes in the far offsets are more sensitive to poisson's ratio variations. As the hydrocarbon presence significantly decreases poisson's ratio (Rutherford and Williams, 1989), it would be possible to associate oil presence to increase of amplitude from Near to Far stack (classe III AVO). In this paper we will show a case where, using only this analysis, would conduct us to a pitfall that was solved through seismic inversion and rock physics analysis.

One of the initial objectives of this project was trying to better understand the seismic signature of three different Miocene uncompacted sands with channel shape. Although all leads, drilled by well 1, well 2 and well 3, were associated with typical class III AVO anomalies, only well 1 sands had some oil content.

Seismic 1-D modeling and fluid substitution using the available wells indicated a polarity inversion of sands seismic reflections associated with the change of saturating fluid (oil to water). As illustrated in Figure 1, compared to the shale, the water bearing reservoir sands were associated with an increase of P-Impedance and poisson's ratio, while the oil bearing sands were associated with a decrease of these two elastic properties. Consequently, the seismic signature of the top of oil sands can be easily confused to the water saturated sands. This behavior explains the amplitude anomalies associated with water sands, causing the pitfall. The interference between the seismic reflections in channel complex also difficult the interpretation.

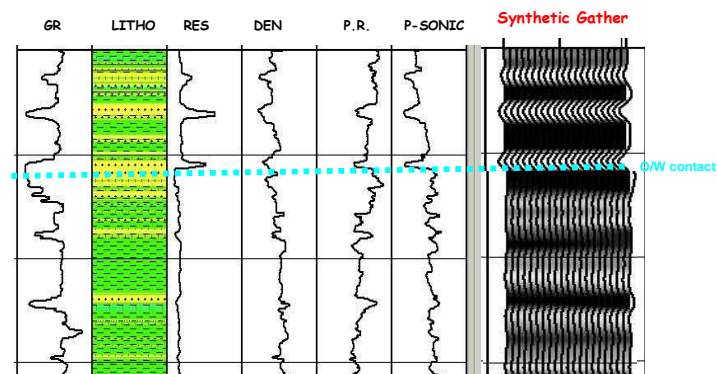


Figure 1: Synthetic gather generated to well 1, using an integrated pulse (layers domain). Oil sands correspond to positive reflections once water sands to negative reflections.

AVO Inversion was used associated with well log analysis, to differentiate the responses from the wells and to infer which zones were oil or water saturated. The main advantages of inversion are that it transforms the data from interface to true layer properties and minimizes tuning effects (deconvolution associated with inversion process) (Ma, 2002; Mallick, 2001).

Feasibility Study

The feasibility study was used to:

- show it is possible, using elastic inversion, to discriminate oil from water sands.
- establish cut-offs that will drive the interpretation of the inversion results.

For the feasibility study we used 3 wells located in the area where the inversion was performed. Only one of these wells found oil (well 1). It was performed the necessary corrections, invasion and washout, and elastic attributes were calculated for these wells.

Rock physics analysis using available well logs found that P-Impedance (IP) and P minus S-Impedance (IP-IS) are the main attributes that discriminates oil sands from brine sands (Figure 2). Fluid substitution using Gassman's equation (Gassman, 1951) was performed in order to investigate the behavior of brine sands if they were oil saturated and vice versa (Figure 3).

From fluid substitution and well log analysis we concluded that it is feasible to discriminate oil from water sands and that using only IP-IS attribute it would be possible to establish a cut off value for oil sand ($IP-IS < 2600 \text{ g/cm}^3 \text{ m/s}$) (Figure 3). The same cut off value is valid when

filtering the log curves to the seismic frequency bandwidth.

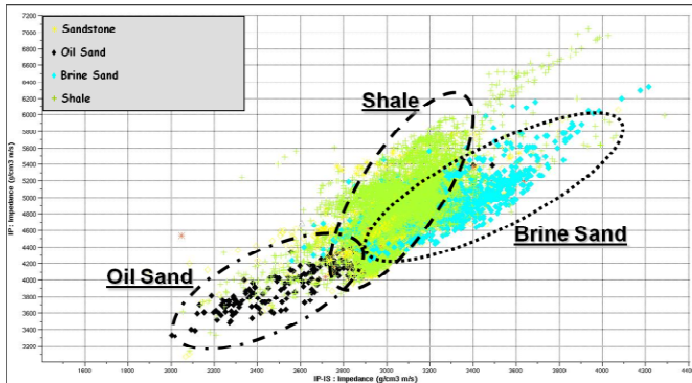


Figure 2: Cross-plot of IP vs. IP-IS using available well logs showing three main clusters: brine sand, oil sand and shale.

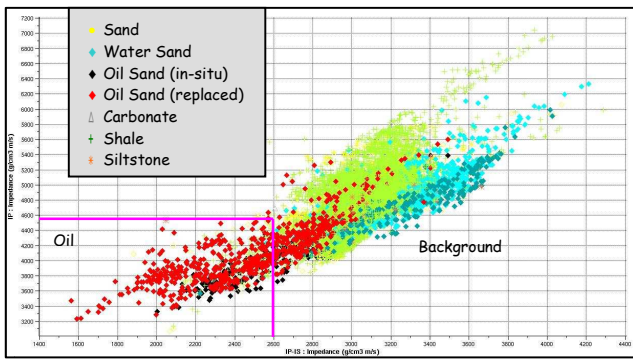


Figure 3: Cross-plot for IP vs. IP-IS when replacing brine to oil in the reservoir interval. In pink we can separate the region with Oil from background.

Our feasibility study analysis shows that replacing brine to oil decreases both Ip and Ip-Is. Therefore, obtaining Ip and Ip-Is from seismic inversion would discriminate oil zones from background.

Simultaneous AVO Inversion - methodology

In this paper, in a model based inversion framework, a set of 4 partial angle stacks were simultaneously inverted using a pre-stack simultaneous inversion based in simulated annealing implemented by Rasmussen (2004) following Ma (2002). The angle range for each partial angle stack is: 02-12, 10-20, 18-28 and 26-36.

Traditionally, separate AVO inversion was performed by independently inverting each available offset or angle stack and obtaining as a result the elastic impedance, which is an angle dependent quantity (Connolly, 1999). Several assumptions were made in the derivation of the elastic impedance concept, such as constant average Poisson's ratio. Furthermore, as elastic impedance is an angle dependent quantity, several elastic impedances from different partial stacks needs to be combined in

order to estimate angle independent quantities such as acoustic impedance, shear impedance and Vp/Vs.

Rasmussen (2004) indicated that the transformation from angle dependent quantities to angle independent quantities increases the misfit between the seismic data and the synthetic, resulting in suboptimal results. Following Ma (2002), Rasmussen (2004) presented a new inversion methodology to directly obtain layer properties by simultaneously inverting a set of angle stacks, and hence avoiding the elastic impedance concept. Figure 3 illustrates the concepts of separate and simultaneous AVO inversion.

In Rasmussen's (2004) methodology, deterministic wavelets for each partial stack are extracted using the available wells and using Aki & Richards approximation (Aki & Richards, 1980) for the reflection coefficient in the well log position (Equation 1). The final wavelet for each partial stack is found by an optimized averaging of the extracted wavelets in each individual well, generating a multi-well wavelet (Figure 5). Lots of tests were performed looking for the wavelet that would generate synthetics that best correlates with the seismic data and gives the best inversion results.

As independent wavelets are estimated for each angle stack, variations in frequency, phase and amplitude between the different seismic input stacks are captured by the wavelets, so there is no need for scaling, phase rotation or frequency balancing of the seismic data.

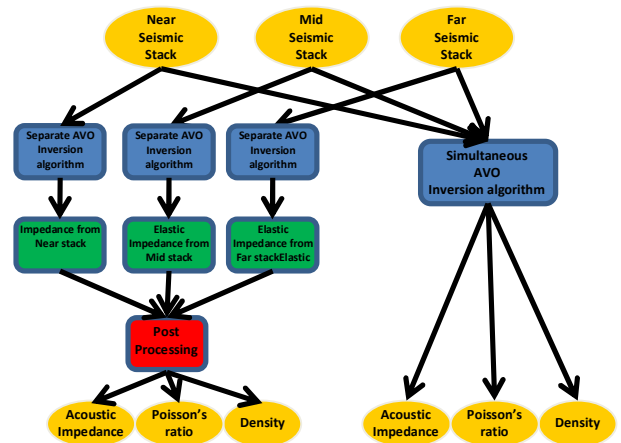


Figure 4: Separate and simultaneous inversion workflows comparison.

$$R = \left(\frac{1}{\cos^2(\theta)} - \frac{8 \sin^2(\theta)}{\exp(y_i + y_{i+1})} \right) \frac{x_{i+1} - x_i}{2} + \frac{8 \sin^2(\theta)}{\exp(y_i + y_{i+1})} \frac{y_{i+1} - y_i}{2} + \left(1 - \frac{1}{\cos^2(\theta)} + \frac{4 \sin^2(\theta)}{\exp(y_i + y_{i+1})} \right) \frac{z_{i+1} - z_i}{2} \quad \text{Eq. 1}$$

Equation 1: Modified equation of Aki & Richards (1981) approximation to Zoeppritz equation (1951) for reflectivity generation used in the model based inversion applied here.

In equation 1, R is the reflectivity output, θ is the average angle of incidence, $x_i = \log(IP_i)$, $y_i = \log(IP_i / IS_i)$ and $z_i = \log(\rho)$. IP , IS and ρ are acoustic impedance, shear impedance and density, respectively.

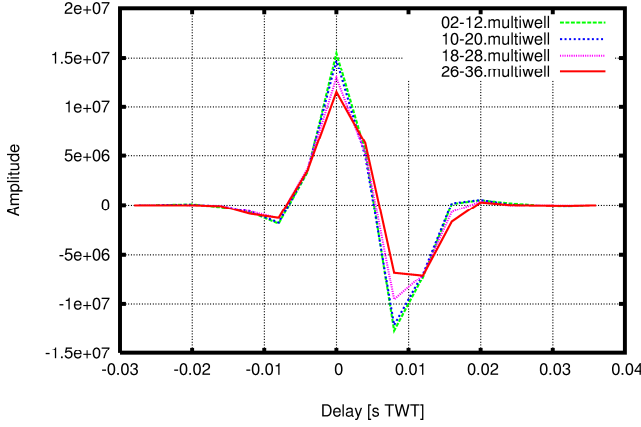


Figure 5: Final Multi-well optimized wavelets extracted using individual wells wavelet.

The inversion engine applied in this work was proposed by Rasmussen (2004) and uses a global optimization algorithm with a non-linear cost function. As described before, it utilizes the modified equation of Aki & Richards (Aki and Richards, 1980) approximation to Zoeppritz equation (Zoeppritz, 1951) to perform the AVO modeling. As shown in equation 1, the parameterization for Aki & Richards approximation has been chosen to be P impedance, P to S impedance ratio and density.

The inversion algorithm used here uses a global optimization algorithm based in simulated annealing to minimize the cost function showed in equation 2 below:

$$Z = \arg \min E_{seismic} + E_{prior} + E_{horizontal} + E_{vertical} \quad \text{Eq.2}$$

Equation 2: Cost function used in the simultaneous inversion applied here.

Where:

$$E_{seismic} = w_1 \sum_{x,y,t} [d(x,y,t) - w(t) \times r(x,y,t)]^2$$

$$E_{prior} = w_2 \sum_{x,y,t} \{ \log[Z(x,y,t)] - \log[Z_{prior}(x,y,t)] \}^2$$

$$E_{horizontal} = w_3 \sum_{x,y,t} \{ \log[Z(x,y,t)] - \log[Z(x \pm 1, y \pm 1, t)] \}^2$$

$$E_{vertical} = w_4 \sum_{x,y,t} \min[r(x,y,t)^2, r_0^2]$$

In equation 2 above, $d(x,y,t)$ is a seismic data sample, $w(t)$ is the estimated wavelet, $r(x,y,t)$ is the reflectivity given by equation 1, $Z(x,y,t)$ is the

impedance contrast value at a certain sample, $Z_{prior}(x,y,t)$ is the impedance contrast value from the initial or prior model and r_0 is the threshold value for valid reflection coefficient.

Yet, in the equation 2 the parameters w_i are penalties associated to each constrain in the cost function. w_1 controls to what degree differences between the synthetic seismic and the seismic data are penalized. w_2 controls to what degree deviation of the estimated impedance model from the prior model is penalized. w_3 controls to what degree horizontal variations in the impedance model are penalized and w_4 controls the definition of significant reflectors.

Simultaneous AVO Inversion - Results

Using a set of 4 angle stacks and the wavelets showed in Figure 5, the simultaneous inversion methodology described earlier was applied in order to estimate IP and IP-IS, according to our feasibility study.

In order to obtain absolute rock properties values, it is necessary to add low frequency information in the inversion engine. In this case, after seismic frequency content analysis (Figure 6), we chose to compensate the seismic for frequencies lower than 10 Hz.

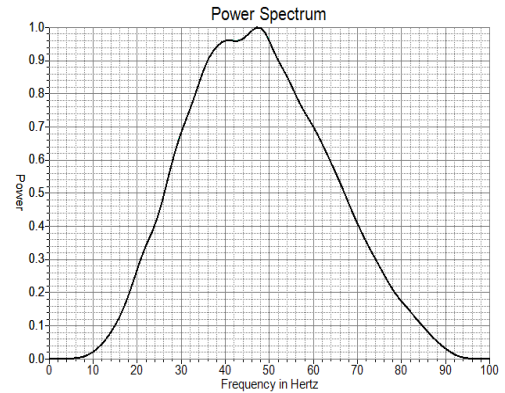


Figure 6: Power spectrum extracted using a cross correlation method. For this case, we chose to compensate for frequencies lower than 10 Hz.

The quality control of the inversion results is done by comparing each property from the inversion algorithm with the corresponding well logs curves. In general, a high pass filter is applied to the well logs to remove the inherent high frequency. Figure 7 to 12 compares the inversion results with well log curves in the available wells. The low frequency model used is also inserted.

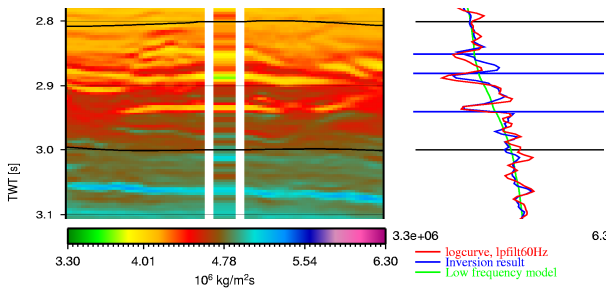


Figure 7: Acoustic impedance inversion result compared with high pass filtered well log curve for well 1. Red: log curve. Blue: inversion result. Green: low frequency model.

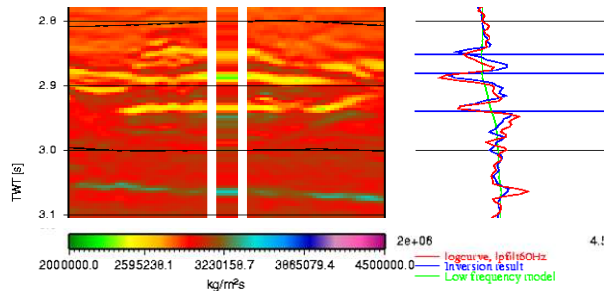


Figure 8: IP-IS inversion result compared with high pass filtered well log curve for well 1. Red: log curve. Blue: inversion result. Green: low frequency model.

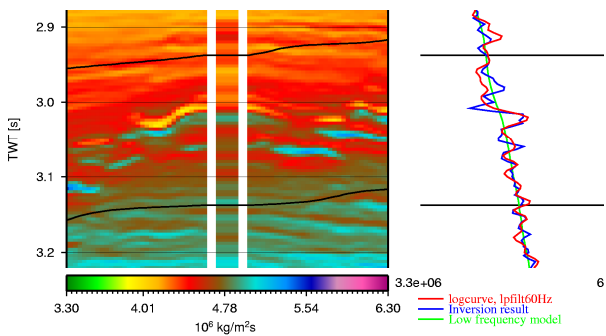


Figure 9: Acoustic impedance inversion result compared with high pass filtered well log curve for well 2. Red: log curve. Blue: inversion result. Green: low frequency model.

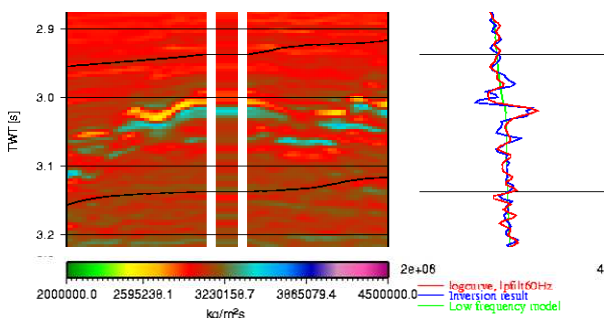


Figure 10: IP-IS inversion result compared with high pass filtered well log curve for well 2. Red: log curve. Blue: inversion result. Green: low frequency model.

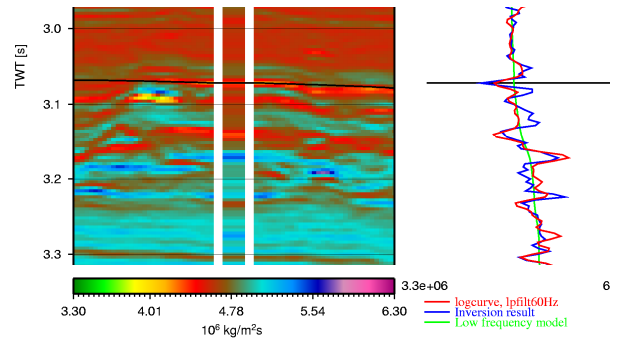


Figure 11: Acoustic impedance inversion result compared with high pass filtered well log curve for well 3. Red: log curve. Blue: inversion result. Green: low frequency model.

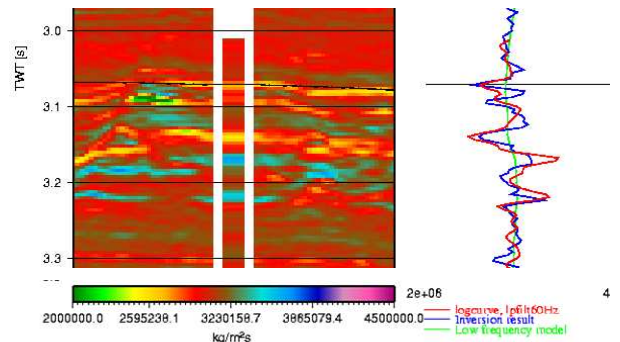


Figure 12: IP-IS inversion result compared with high pass filtered well log curve for well 3. Red: log curve. Blue: inversion result. Green: low frequency model. For this well there is no shear measurement in the zone of interest.

The inversion results show good match with measured well log curves. It is important to remember that in seismic inversion workflows the rock properties are extracted only from seismic amplitudes. The well information is only used indirectly in the inversion algorithm, only in the wavelet extraction and in the low frequency model building. Therefore, comparing the calculated rock properties extracted only from seismic amplitudes with measured well log curves can give a good estimate on the inversion algorithm accuracy and in the quality of the seismic inversion.

Results integration

After feasibility analysis and elastic inversion, it is necessary to interpret, in an integrated way, all the available information. This was done using the cut off values obtained from rock physics analysis.

In Figure 13 it is possible to see a map built over the surface that crosses the first reservoir sands from well 1 and well 2. The cutoff defined in Figure 2 was used to compose the color scale, enhancing what would possibly be the oil sands. For well 3 the same analogy is not valid because the surface does not cross the reservoirs.

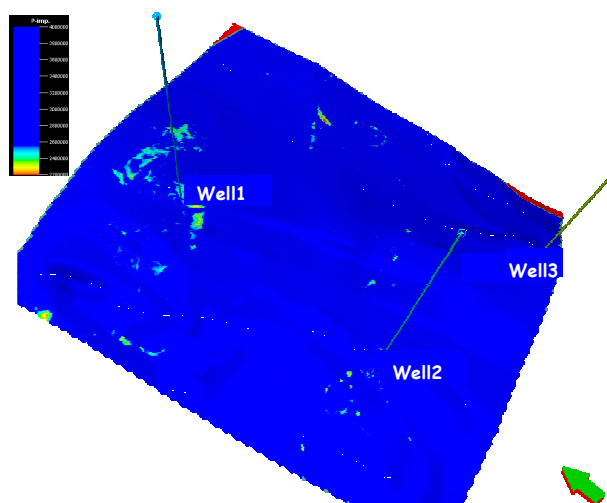


Figure 13: Surface crossing the reservoir interval at well 1 and 2. Rock properties derived from seismic inversion are projected in this map. The color scale follows cut off values defined in figure 2.

Figure 14 (a) e (b) illustrates the gain obtained from the use of inversion to understand the seismic responses of these sand complex channels. In (a) it is shown an amplitude probe over Far stack, showing two strong amplitude anomalies with channel geometry. In (b) is shown another probe obtained applying the cutoffs to IP and IP-IS together. As the reader can see, in (b) it is possible to differentiate the seismic signatures of the leads at well 1 and well 2, and associate this differentiation with different fluid content.

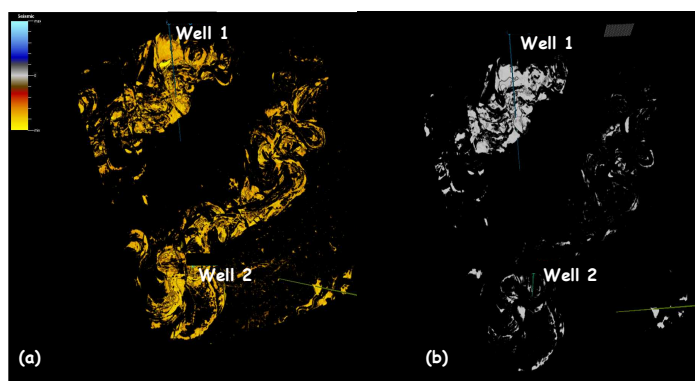


Figure 14: (a) Far amplitude probe with opacity and (b) captured sub-volume using IP and IP-IS cutoffs.

A conventional approach, just looking for amplitude anomalies or even typical AVO III anomalies, would in some situations lead the interpreter to a misinterpretation. So, this kind of study has a big impact over reservoir evaluation, reducing exploratory risks.

Conclusions

We have shown a case where seismic inversion combined with rock physics analysis reduced the pitfall risk associated with AVO anomalies in deep water channels. The inversion results integration with well log analysis allowed to differentiate oil (well 1) from water sands (wells 2 and 3), solving the pitfall that was initially identified in the area. This success is associated with the tuning effect reduction and the data domain change (interface to layer) intrinsic to inversion process.

Acknowledgements

We would like to thanks to Ricardo Tarabini, Fernando Barbosa and Carlos Rodriguez, all of them Petrobras consultants, for their contributions for this paper.

Bibliography

- Aki, K., and Richards, P. G., 1980, Quantitative seismology: Theory and methods: W. H. Freeman and Co
- Castagna, J. P., Batzle, M. L., and Kan, T. K., 1993, Offset-dependent reflectivity—Theory and practice of AVO Analysis: Soc. Expl. Geophys., 135–171
- Connolly, Patrick, 1999, Elastic Impedance, The Leading Edge, April.
- Rasmussen, Klaus B., Pedersen, Jacob M., 2004, Simultaneous Seismic Inversion, EAGE, 66th Conference and Exhibition.
- Rutherford, Steve R., Williams, Robert H., 1989, Amplitude-versus-offset variations in gas sands. Geophysics, Vol. 54, No. 6.
- Ma, X-Q, 2002, Simultaneous inversion of pre-stack seismic data for rock properties using simulated annealing. Geophysics, 67, 1877-1885.
- Mallick, Subhashis, 2001, AVO and elastic impedance, The Leading Edge, October.
- Zoeppritz, K., 1919, Erdbebenwellen VIII B, Über Reflexion und Durchgang seismischer Wellen durch Unstetigkeitsflächen: Gottinger Nachr., 1. 6684.